Buried UXO Classification Using the Polarization and Resonance

Chi-Chih Chen

The Ohio State University ElectroScience Laboratory
1320 Kinnear Road, Columbus, OH 43212
TEL: (614) 292-3403
FAX: (614) 292-7297
E-mail: Chen.118@osu.edu

Category: Detection Technology Section

Abstract **- This paper discusses the background and the feasibility of using the complex natural resonance (CNR) and polarization signatures to classify buried unexploded ordnance (UXO). Natural resonance feature has been used for UXO classifications with a reasonable success in easy soils. The polarization feature is included here as another classification feature to help reduce the large number of false alarms caused by shrapnel.**

A. Introduction

When a conducting target is illuminated by a radar source, it scatters the electromagnetic energy through reflection, diffraction and resonance mechanisms. Each scattering mechanism contains target signatures that can be used for radar target recognition. Some signatures may have advantages over the other for some applications. Choosing proper signatures is indeed the most challenging problem in target recognition. This paper discusses the use of natural resonance and polarization signature for classifying buried unexploded ordnance (UXO). The medium will be assumed to be isotropic and homogeneous throughout this paper.

The natural resonance modes of a conducting target are excited when the incident electromagnetic fields induce currents on a conducting surface. The finite surface area limits the current flow and causes it to flow back and forth on the body. When the frequency coincides with the period of the oscillation of the induced currents, strong resonance occurs. The resonant currents also experience damping due to radiation. Such resonant radiation is then detected by radar as damped sinusoids. The natural resonant modes can be used for the target classification by relating the resonant wavelengths to the target structures, such as fuselage and wings. Reasonable success of applying the natural technique to classify buried UXOs has been achieved for easy medium [1]. For buried UXO's, proper correction must be done to include the effect of the soil.

The electromagnetic fields scattered from a buried target have certain polarization properties related to the shape, composition and orientation of the target. This paper will be focussed on the backscattering case where the transmitting and receiving antennas are either co-located or the same one. "Co-polarized" data are measured when both the transmitting and receiving antennas have a same polarization. On the other the "cross-polarized data" are collected when the transmitting and receiving polarizations are orthogonal to each other. Both co-polarized and cross-polarized data must be recorded to obtain complete polarization information.

Most UXOs have elongated bodies that make them resonate strongly and the backscattered fields linearly polarized in the axis direction. The scattered fields polarized along the UXO axis direction will be referred to as the "primary fields" hereafter. As the diameter of an UXO increases, the "secondary fields", polarized perpendicularly to plane formed by the UXO axis and the incident waves, also intensify. The primary and secondary axes are indicated in Figure 1. It will be shown that the UXO length-to-diameter (L/D) ratio can be obtained from the relationship between the primary and secondary fields.

B. Natural Resonance Signature

A well known advantage of using the CNR signature for target classification is its orientation independence. Its magnitude, however, is a function of orientation and excitation source. Most UXO's have simple geometry that can be easily modeled such that their CNR's can be predicted. Figure 3 plots the free space CNR extracted from four UXO numerical model data. Th CNR's are extracted using the TLS-Prony method [3]. The four actual UXO types (designated as #2075 , #2077, #2082 and #2083) are also shown in Figure 4. From Figure 3, the fundamental resonant frequencies for #2075, #2077, #2082 and #2083 are found to be 450 MHz, 620 MHz, 110 MHz and 110 MHz, respectively. These lead to the estimated lengths of 13", 9.5", 54" and 30", respectively. The actual "front-to-tail" lengths are 11.3",7.5",39" and 25". The CNR predicted length from tends to be longer than the actual length. This is due to the fact that the induced currents are flowing along the curved surface as well as the two end surfaces. This extra path length causes the CNR estimated length longer than the actual "front-to-tip" length. The error in less for thin UXOs and greater for fat UXO. The UXO with tail fins, such as #2082, has the biggest length difference.

When a UXO is buried, its CNR's are modified by the soil electrical properties according to Eq. (1) derive by Baum [2].

$$s = -\frac{\sigma}{2\varepsilon_0} + \left[\left(\frac{\sigma}{2\varepsilon_r} \right)^2 + \frac{s_0^2}{\varepsilon_r} \right]^{1/2}, \quad (1)$$

where $s_0 = \alpha_0 + j\omega_0$ is the free space CNR with α_0 and β_0 being the damping factor and the angular resonant frequency, respectively. s is the new CNR in the medium. This modification effect can be illustrated by Figure 2 where a CNR pole (dark circle) is moved to different locations according to various dielectric constant and conductivity. For low conductivity soil, both the resonant frequency and the damping factor are approximately inversely proportional to the dielectric constant. As the conductivity increases, the pole location is severely distorted. It requires the knowledge of the soil property and Eq. (1) to recover the original pole.

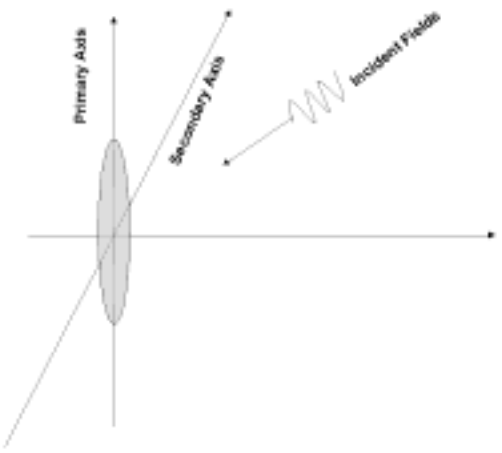

Figure 1 The primary and secondary fields of UXO scattering.

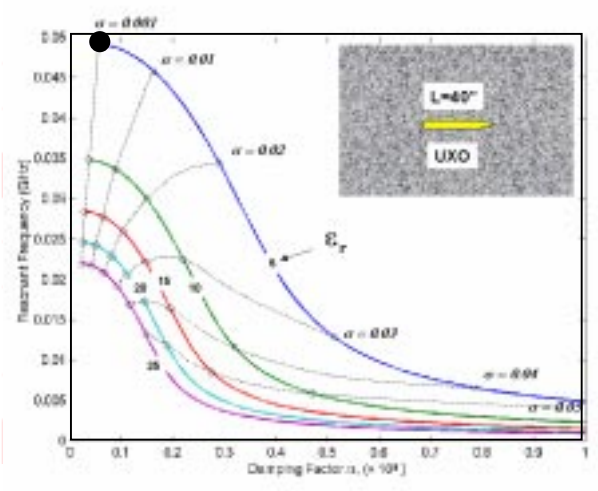

Figure 2 The variation of the resonant frequency and damping factor as a function of soil dielectric constant, ε_r, and conductivity, σ, as predicted by Eq. (1).

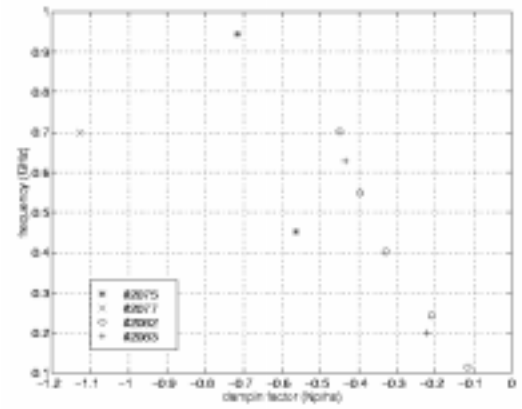

Figure 3 The CNRs extracted from full-scale UXO numerical model data.

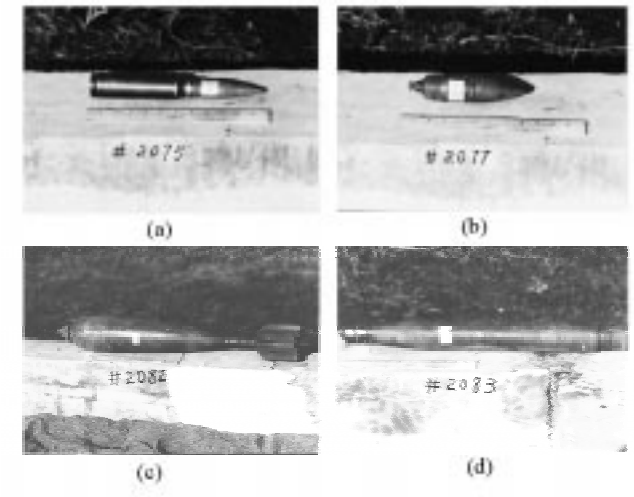

Figure 4 Photos of the UXOs used for numerical modeling and CNR extractions.

C. UXO Polarization Signature

The backscattered fields can be expressed by the scattering matrix, $\overline{\overline{S}}$, and the incident fields, E^i, as

$$\begin{bmatrix} E_v^s \\ E_h^s \end{bmatrix} = \frac{e^{-jkr}}{r} \overline{\overline{S}} \begin{bmatrix} E_v^i \\ E_h^i \end{bmatrix}, \qquad (2)$$

where $\overline{\overline{S}} = \begin{bmatrix} s_{vv} & s_{vh} \\ s_{hv} & s_{hh} \end{bmatrix}$ and the subscripts ,h and v, indicate the antenna orientations.

The scattering matrix can then be diagonalize using a standard eigenfunction expansion technique. That is

$$\overline{\overline{S}} = \sum_{j=1}^{2} \lambda_j \hat{e}_1 \hat{e}_{2,} \qquad (3)$$

where $\hat{e}_j$ are the eigenfunctions used to diagonalize the scattering matrix. The final diagonal matrix contains the eigenvalues, λ_j, i.e.

$$\overline{\overline{D}} = \begin{bmatrix} \lambda_1 & 0 \\ 0 & \lambda_2 \end{bmatrix}. \qquad (4)$$

This diagonalization procedure can be considered as an alignment procedure such that the backscattered fields are decomposed into the components that are aligned to the target's primary and secondary sacttering axes. The directions of these axes are exactly the directions of eigenfunctions. The scattering amplitudes along these axes are determined by the corresponding eigenvalues.

Figure 5 illustrates the difference between the measurement coordinate and the scattering coordinate. The measurement coordinates are determined by the transmitting and receiving antenna orientations. The scattering coordinate is defined as the target-preferred scattering polarizations. Assuming that the scattering coordinate is obtained by rotating the measurement coordinate an angle, β, then Eq. (3) can be explicitly written as

$$\overline{\overline{S}} = \lambda_1 \begin{bmatrix} \cos^2\beta & \cos\beta\sin\beta \\ \sin\beta\cos\beta & \sin^2\beta \end{bmatrix} + \lambda_2 \begin{bmatrix} \sin^2\beta & -\sin\beta\cos\beta \\ -\cos\beta\sin\beta & \cos^2\beta \end{bmatrix}. \qquad (5)$$

Eq. (5) can then be decomposed into a rotationally symmetric component and a linearly symmetric component, as shown in Eq. (6).

$$\overline{\overline{S}} = \frac{\lambda_1 + \lambda_2}{2} \begin{bmatrix} 1 & 0 \\ 0 & 1 \end{bmatrix} + \frac{\lambda_1 - \lambda_2}{2} \begin{bmatrix} \cos 2\beta & \sin 2\beta \\ \sin 2\beta & -\cos 2\beta \end{bmatrix}. \qquad (6)$$

The first term corresponds to the rotationally symmetric component since the two eigenvalues are equal. The matrix in the second term is recognized as a mirror transformation that transforms a point into its mirror point with respect to a line oriented at β direction, i.e., $\hat{e}_1$ direction in Figure 5. Therefore, the second component corresponds to the scattering component that has linear symmetry

This interesting discovery leads to the definition of the *degree of linear polarization* (DLP). That is

$$DLP = \frac{|\lambda_1 - \lambda_2|}{|\lambda_1 + \lambda_2|}. \qquad (6)$$

DLP is an important parameter that measures the degree of linearity in the scattered fields. DLP can be defined in frequency domain as well as time domain depending on the application. It should be noted that a similar definition has been existing in the literature [4]. However, the author believes that the approach used in this paper provides more physical insight.

Figure 6 illustrates how DLP is related to the geometry of a scattering target. Two-wire targets with different length and angle combinations represent targets of different degree of linearity. As the overall geometry becomes more linear, the DLP approaches to 1. Notice that most UXOs would have than larger DLP number than that from the clutter, such as voids, rocks, UXO shrapnel.

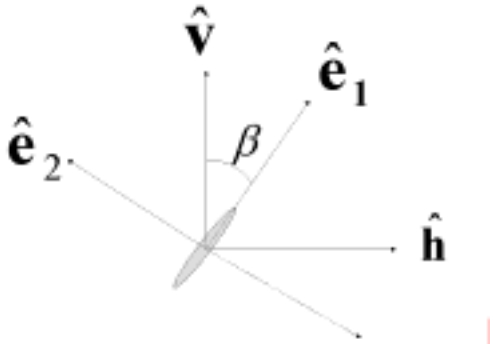

Figure 5 The measurement axes (v,h) and target's primary and secondary axes (e_1,e_2).

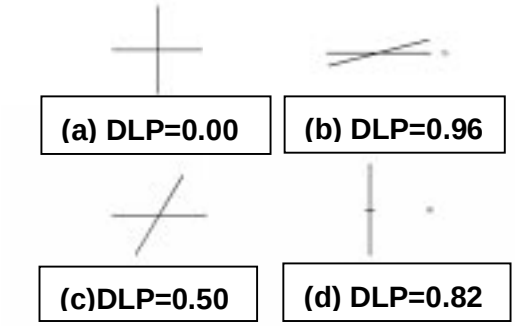

Figure 6 Examples of different DLPs, for various two-wire scatters.

Figure 7 plots the calculated the primary and secondary backscattered fields, shown by the thin and thick lines, respectively, for an 18" long conducting cylinder in free space. The diameter is 6". The frequency range is from 50 to 550 MHz. Since the transmitting and receiving polarizations are aligned to the cylinder's primary and secondary axes. The backscattered fields are proportional to the eigenvalues.

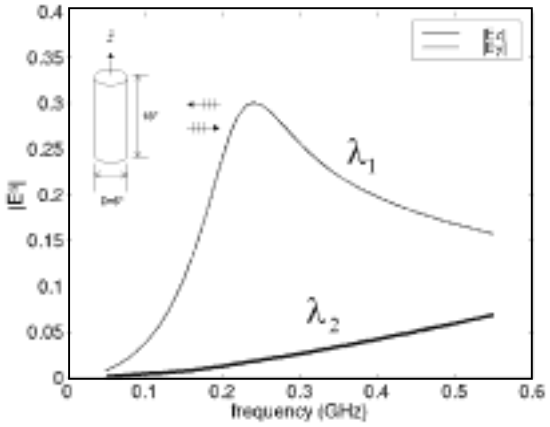

Figure 7 The calculated primary and secondary backscattered fields for a conducting cylinder in free space.

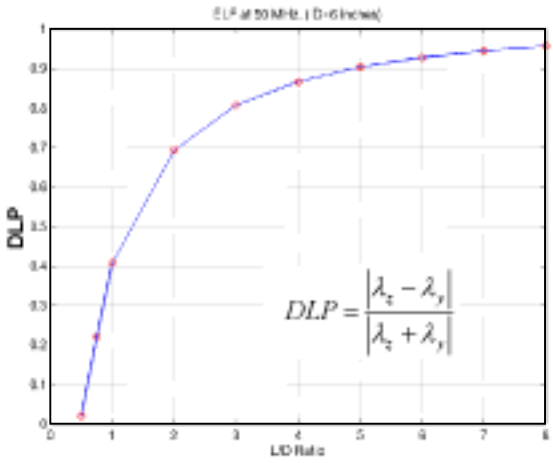

Figure 8 The relationship between the degree of linear polarization (DLP) and the L/D ratio for conducting cylinders.

First, it is observed that the primary field is stronger than the secondary field. Both the primary and secondary fields increase with the frequency since the cylinder becomes larger in wavelength at higher frequency. However, if the cylinder is buried in the soil, more energy will be absorbed by the soil at higher frequency. An additional resonance peak is also observed at approximately 240 MHz in the primary field data. This resonant frequency corresponds to a resonant length of 24.6", which is close to the 24" physical distance from center of the one end-cap to another one.

For frequency far below the resonant frequency of the primary field, there is simple relationship between the L/D ratio and the DLP as shown in Figure 8. The frequency used to obtain Figure 8 is 50 MHz. As the L/D ratio increases, the cylinder becomes thinner the backscattered fields become highly polarized, and thus the DLP approaches to one.

The polarization feature can also be obtained from time domain data. Figure 9 plots calculated radar data in time-domain from a full-scale UXO numerical model shown in Figure 10. The primary and secondary fields are plotted in solid and dashed lines, respectively. Similar to the previous conducting cylinder and most UXO's, only the primary fields contain resonant radiation. Such resonant signal creates a tail at late-time. The DLP and LD ratio at the early-time, as shown in t=0 ns in Figure 9, would have a relationship similar to Figure 8. If the DLP is calculated at late-time, the DLP would be close to 1 since λ_2 vanishes. This is a very important in separating UXO from other clutter since most clutter do not resonant in the frequency range interested.

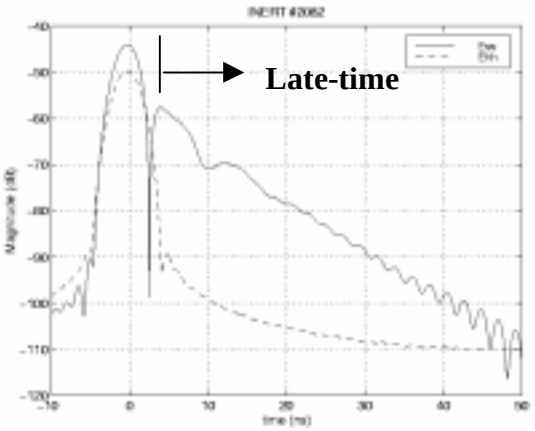

Figure 9 The time-domain data associated with Figure 10. The primary and secondary fields are shown by the solid and dashed lines, respectively.

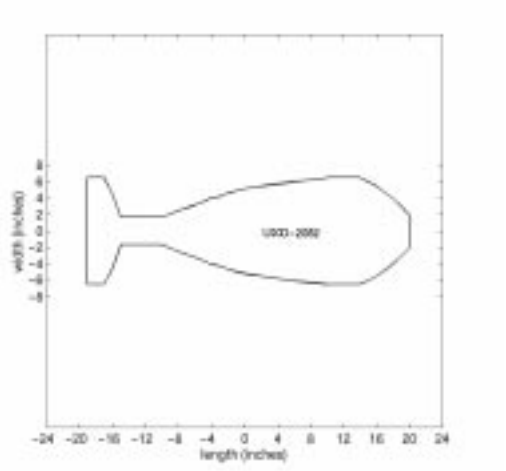

Figure 10 The Full-scale UXO numerical model used to calculated the radar data in Figure 9.

D. Conclusion

Two complex natural resonance and linear polarization features associated with UXOs were discussed. These features could be used to separate true UXOs from many false alarm sources that do not share the same features. Theoretical examples using full-scale numerical models were provided to demonstrate the extraction of CNR and polarization features. The links between these features to the UXO length and UXO length-to-diameter were also presented.

The CNR classification technique is particular useful in identifying large UXOs whose resonant lengths are significantly longer than most shrapnel. As discussed, the major difficulty in applying the CNR technique for UXO classification is the ability to calibrate the CNRs to obtain the equivalent free-space CNRs that ate then used to estimate the UXO length. The variations in the soil property due different soil types and moisture content affect the calibration accuracy. In a sandy medium, such calibration is quite feasible.

The linear polarization feature of UXO presents another useful tool for UXO classifications. This feature is due to the UXO's unique long bodies that are different from most false alarms. As shown in this paper, this feature also exists in the low frequency region where good penetration can be achieved. The LD ratio can be estimated from the polarization feature directly. It was also shown that the linear polarization feature can be obtained in the time domain where one can take the advantage of UXO's resonance property as well.

E. References

[1] C.-C. Chen and L. Peters Jr., "Buried unexploded ordnance identification via complex natural resonances,", IEEE Trans. Antennas. Propagat., vol. AP-45, pp.1645-1654.
[2] C. E. Baum, "The SEM representation of scattering from perfectly conducting targets in simple media," Phillps Lab., Kirtland Air Force Base, Interaction Note 492, Apr.1993.
[3] M. D. A. Rahman and K.-B. Yu, "Total least square approach for frequency estimation using linear prediction," IEEE *Trans. Acoust., Speech Signal Processin*g, vol. ASSP-35, pp.1440-1454, Oct., 1987.
[4] W. L. Stutzman, "Polarization in Electromagnetic Systems," 1993, Artech House,Boston.